3D Printing for microfabrication and mechanical stress characterization in flexible electronics

A. G. Gonzalez^a, O. Obregon^b, S. Ceron^b, S. Soto^b, and M. A. Dominguez^{b,*}

^aInstituto Tecnológico Superior de Ciudad Serdán, Puebla 75520, Mexico.

^bCentro de Investigaciones en Dispositivos Semiconductores, Instituto de Ciencias,

Benemérita Universidad Autónoma de Puebla, Puebla 72570, Mexico.

*e-mail: miguel.dominguezj@correo.buap.mx

Received 13 June 2025; accepted 19 June 2025

In this work, the application of 3D printing for microfabrication and mechanical stress characterization in flexible electronics is presented. The 3D printing method used is fused deposition modeling with polylactic acid (PLA) filament as an eco-friendly alternative. For mechanical stress characterization, a 3D device is designed to be adapted to the requirements of flexible samples showing accuracy, versatility and easy implementation in any probe-station. For microfabrication, a PLA 3D shadow mask is used to transfer silver patterns to flexible substrates such as Polyethylene Terephthalate (PET) and photographic paper. A systematic study to evaluate the mechanical stress in the silver patterns is conducted using the 3D printed devices previously designed. The silver film is evaporated using a thermal evaporating coater. Finally, to demonstrate a flexible Printed Circuit Board (PCB) application, a silver path evaporated on PET substrate is used as a transmission line for a sine electrical signal. The flexible PCB exhibits a reliable electrical operation even when the substrate is bent.

Keywords: Flexible electronics; Microfabrication; Mechanical stress; bending test.

DOI: https://doi.org/10.31349/RevMexFis.71.061003

1. Introduction

Recently, flexible electronics is gaining attention in the research community due to several novel applications for wearable and Internet of Things (IoT) technologies, since cardiovascular healthcare monitoring, electrochemical sensors, flexible displays, flexible integrated circuits, among others [1-4]. Flexible electronics have the advantage of stretchability, bendability, and/or conformability thanks to the use of flexible substrates such as Polyethylene Terephthalate (PET), Polyethylene Naphthalate (PEN), Thermoplastic Polyurethane (TPU), cellulose paper and especially polyimide [3,5,6]. The main challenge in flexible electronics is the mechanical stability, since the devices are bent and stretched several times which affects their electrical operation [1,3,7]. The bending tests are necessary to extract parameters while the device is in operation. However, several authors reported in literature bending tests using glass tubes or metal/plastic rods with radius selected randomly, not by experimental design [1,2,4,6,8-11]. This limits the mechanical stress characterization since varying systematically the tensile radius becomes inaccurate, complex and/or expensive.

On the other hand, 3D printing technology has revolutionized both research and industry fields due to low-cost and ease of operation. The most widely 3D printing method used is fused deposition modeling (FDM), where an extruder mechanism is used to deposit layers of fused thermoplastic material [12-14]. Also, 3D FDM printing offers non-toxic materials and rapid prototyping [12]. Different thermoplastic filaments can be used in 3D FDM printing, where the polylactic acid (PLA) and the copolymer acrylonitrile butadiene styrene (ABS) are the most widely used [12]. PLA filaments

offer the advantage of a non-toxic biodegradable material derived from natural sources [12]. Although there is an interest in the use of other biobased and biodegradable filaments [15], different strategies are under development to strengthen PLA in biomedical and agriculture applications [15]. Moreover, PLA is considered a reliable option to develop conductive filaments in biosensors [16]. Another great advantage of 3D printing is the wide range of designs and applications due to the digital modeling of a 3D piece by computer aided design (CAD) software.

It is of interest that 3D printing may find a reliable use in flexible electronics microfabrication, with the advantages mentioned earlier, can be used as a fast-prototyping tool for Printed Circuit Boards (PCBs) and flexible devices. Usually in microfabrication of electronic devices in rigid substrates, such as silicon wafers and glass, photolithography and wet/dry etching processes are widely used to transfer patterns in order to fabricate the device [17,18]. A shadow mask can be an alternative when a material can be damaged by photolithography or etching processes, or even to make faster the fabrication process [18]. However, the fabrication of a shadow mask implies the use of photolithography and wet etching processes as well. For these reasons, low-cost 3D printed shadow masks have been explored as an alternative to transfer metal patterns in microfabrication [17-20]. In Ref. [17], an ABS shadow mask was 3D printed to transfer a 100 nm-thick copper pattern on glass substrates using a high vacuum thermal coating equipment. In Ref. [18], an ABS 3D printed shadow lift-off mask was printed directly onto the Si wafer. Ti/Au films were sputtering through the 3D printed mask to transfer the pattern.

In this work, the application of 3D printing for micro-

fabrication and mechanical stress characterization in flexible electronics is presented. The 3D printing method used is FDM with PLA filament. For mechanical stress characterization, a 3D device is designed to be adapted to the requirements of flexible samples showing accuracy, versatility and easy implementation in any probe-station, in order to address the limitations reported in literature by using random tensile radius. For microfabrication, a PLA 3D shadow mask is used to transfer silver patterns to flexible substrates such as PET and photographic paper, offering a low-cost, fast fabrication and reliable alternative. Moreover, with the use of PLA the 3D shadow masks become a biodegradable option. The silver film is evaporated using a thermal evaporating coater.

2. Experimental section

In flexible electronics applications, it is of great relevance to establish the effect of deformation on electrical performance, and it is also important to determine the critical deformation at which the flexible device electrically fails. Usually, the bending effects are calculated considering the bent of the sample fitted in a cylinder of radius r. Thus, the tensile radius, which is inversely proportional to the strain, is used according to the Eq. (1) [21].

$$Strain(\%) = ((ST + TT)/2r) \cdot 100, \tag{1}$$

where ST is the substrate thickness, TT is the thin-film thickness and r is the tensile radius of the substrate. Figure 1 shows a schematic representation of Eq. (1).

The FDM Ender-6 3D printer from Shenzhen Creality 3D Technology Co., Ltd was used. Polylactic acid (PLA) filament was used as a biodegradable alternative. The general print settings were Quality: 0.1 mm, Infill: 80%, Top/bottom pattern: zig zag. The printing temperature was 200°C and the bed temperature 60°C. The Creality slicer 4.8.2 software was used. The printing time was 5 min.

For the use of 3D printing for microfabrication, a shadow mask was designed with patterns at different scales in order



FIGURE 1. Schematic representation of the tensile radius in a flexible sample.

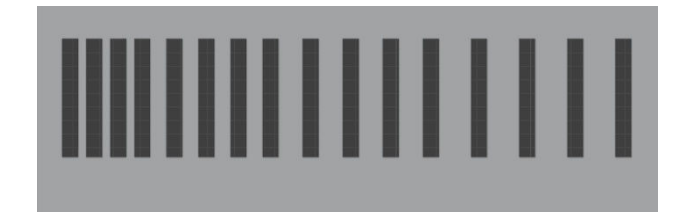


FIGURE 2. Shadow mask design with patterns at different separation.

to find the minimum length resolution in the printed mask. The pattern consists in rectangular shapes with a width of 10x and length of 2x, with a separation of x to 4x. Initially, x was used at 100 μ m and was increasing until the minimum length was found in the 3D printed mask. Figure 2 shows the shadow mask design. To evaporate the silver film a thermal evaporating coater (GSL-1700x-SPC2, MTI Corp.) was used. PET and photographic paper substrates were used. The electrical measurements were made using a function generator (UNI-T model UTG9005C) and an oscilloscope (UNI-T model UT-81B). An electrical signal from 10 to 200 kHz and 4 V amplitude was used. There is no specific reason to choose the frequency and amplitude parameters for the electrical signal, since it is just for an application example. A sine signal is closer to the typical signals used in analog electronics, although triangular and square signals were also evaluated. All the measurements were performed at room temperature and ambient conditions.

3. Results and discussion

Figure 3 shows a basic design with a fixed tensile radius following the schematic representation of Fig. 1. As can be seen in Fig. 3a), the top surface of the printed device follows the tensile radius making it easy to fit the sample to the device. Figures 3b), 3c) and 3d) show different views of the design. One advantage of this design is that the height and length can be adjusted to fit the size of the sample, while the top surface can maintain the same tensile radius. These features offer versatility and accuracy in order to characterize systematically different strain values, since a variety of different tensile radius can be designed for the same flexible device.

Figure 4a) shows a set of 3D printed devices with a variety of different tensile radius. In these printed devices, the length of the device was fixed at 2.5 cm to fit our samples. Figure 4b shows the use of the printed device with a sample of electronic devices fabricated on PET substrate. As can be seen in fig. 4b, the printed device can be easily adapted to any probe-station for characterization while the electronic device is in operation. In comparison with the reported in literature, the 3D printed device can have specific parameters to accurately calculate the strain in any kind of flexible sample. Therefore, this design offers a reliable alternative to study the strain-dependent characteristics in flexible electronics by

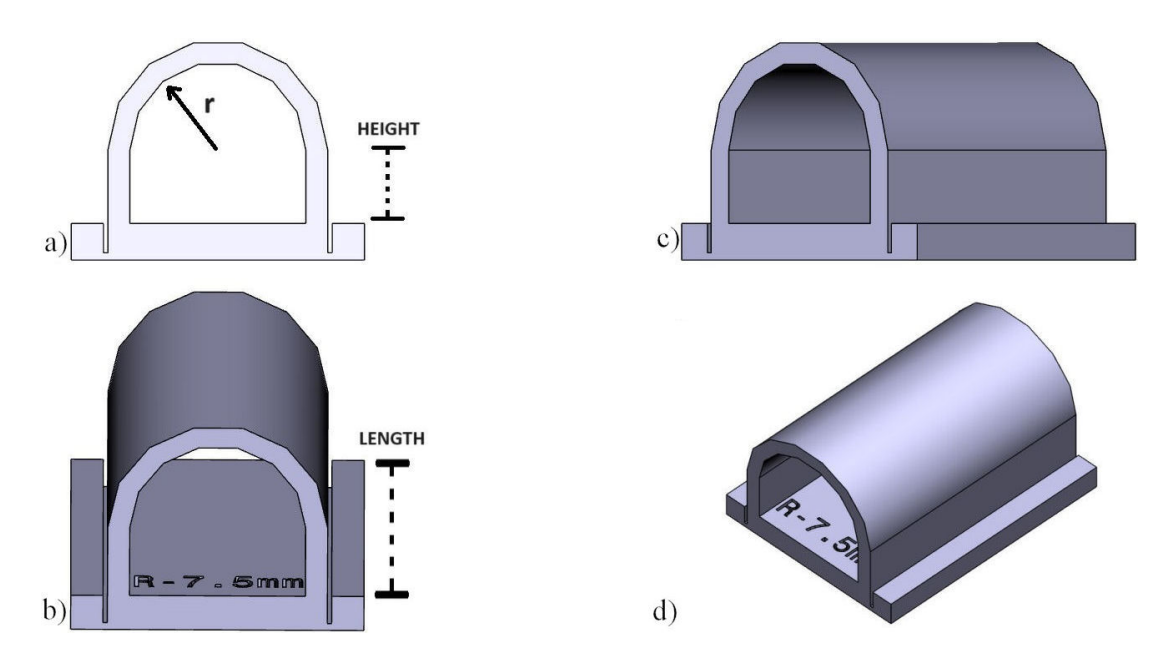


FIGURE 3. Basic design with a fixed tensile radius. a) front view, b) Z-axis rotated view, c) Y-axis rotated view, d) 3D modeled device.





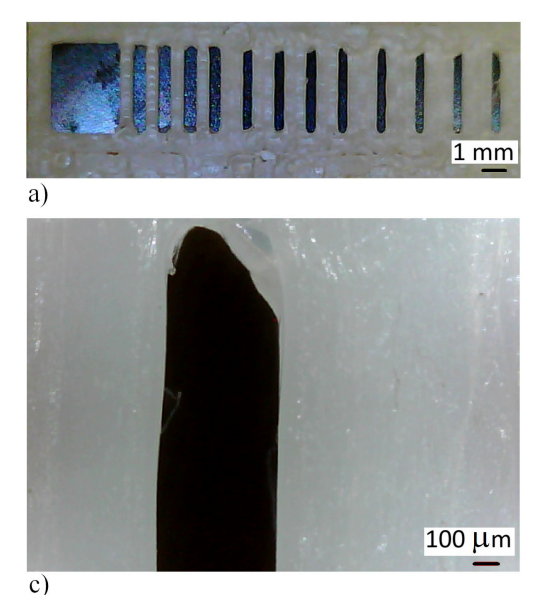
FIGURE 4. A set of printed devices with a range of different tensile radius. a) Printed devices, b) printed device adapted to a probe-station for characterization.

varying systematically the tensile radius. For the case to evaluate a different shape, such as a concave position, this design can be adapted to meet the specific requirements.

According to the literature, a few bending machines have been reported [3,7,22]. Some of them consist of one fixed plate and a second movable plate to adjust the tensile radius of the flexible devices by bringing the plates closer together. Although these machines are useful, they can be large and complex to integrate into a probe-station. In Ref. [23], the authors reported the use of a commercial three-point flexure testing system, which can offer reliable accuracy, but also the inconvenience of high-cost, large-area and complexity to integrate it within a probe-station. In other works, it has been reported home-made bending systems to characterize the strain by varying the tensile radius [1,21,24-31]. Some of them consist in two fixed plates to hold the sample on both sides, and as the plates get closer, the sample tends to bend, forming a curve to calculate the tensile radius. The main dis-

advantage of these bending systems is the probable inaccurate tensile radius that can be calculated from the curve. Also, they may present high-cost and complexity to integrate them with a probe-station. For these reasons, 3D printing can be a low-cost and reliable alternative to be implemented in the mechanical stress characterization in flexible electronics.

On the other hand, another interesting application of 3D printing in Flexible electronics is microfabrication of PCBs and flexible devices. In Fig. 2 the pattern of different contacts was shown to be 3D printed as a shadow mask. In order to find the minimum optimal resolution, $100~\mu m$ was considered as the minimum length and then, it was increasing until an optimal resolution was found. Figure 5a) shows the 3D printed shadow mask with a non-optimal minimum length of $250~\mu m$. As can be seen, the 3D printer does not have the resolution to print at this scale accurately. The optimal minimum length was found at $600~\mu m$ with a variation of $\pm 10~\mu m$ (16 patterns were evaluated), as shows Fig. 5b). In other pub-



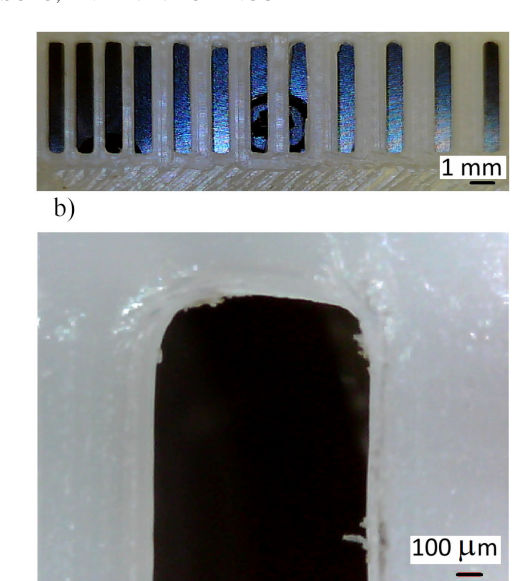


FIGURE 5. 3D printed shadow mask. a) With a minimal length of 250 μ m. b) With an optimal minimum length of 600 μ m. c) Variations in patterns with a resolution lower than the minimum found. d) A well-defined pattern in the 3D printed shadow mask with the optimal minimal resolution found.

lished works the minimum resolution reported was close to 740-870 μm and some novel applications were in the range of millimeters [18,19,32-35]. In Ref. [32], a glucose sensor screen-printed on Algae-based substrates with a minimum spacing between electrodes of 1.2 mm was reported. In Ref. [35], a screen-printed humidity sensor with a dimension of 17×23 mm with a minimum length of 1 mm was reported. This minimal resolution is reliable for Flexible PCBs and may be efficient for fast prototype fabrication of sensors, electrodes and interconnections in flexible electronics. Although not yet for high-density integrated circuits. Figure 5c) shows the variations in patterns with a resolution lower than the minimum found, while Fig. 5d) shows a well-defined pattern in the 3D printed shadow mask with the optimal minimal resolution found $(600\pm10~\mu m)$.

Figure 6 shows the silver evaporated paths on different substrates. Figure 6a) shows the paths in the 3D printed shadow mask for comparison. Figure 6b) shows the silver paths evaporated on silicon wafers, while Figs. 6c) and 6d) show the silver paths on PET and photographic paper substrates, respectively. Figure 7 shows the current-voltage measurements of the silver paths. All measurements exhibit linear and symmetric behavior expected in ohmic contacts. Based on forward and reverse measurements, it can be observed that hysteresis is negligible. These results offer the possibility of using the silver paths as conductive tracks in flexible, recyclable or biodegradable PCBs according to the

substrate used. It is important to mention that current-voltage measurements of Fig. 7 are representative of 10 measurements in each substrate.

The set of printed devices of Fig. 4 were used to systematically characterize the mechanical stress in the silver paths, varying the tensile radius from flat position to 7.5 mm. Five tensile radius were selected 17.5 mm, 15 mm, 12.5 mm, 10 mm and 7.5 mm. The resistance was calculated using the ohm's law. Table I shows the summary of the calculated values. The values were calculated from 5 measurements in each printed device and each substrate.

According to the results, the silver paths exhibit very similar resistances from flat position to a bent position with a tensile radius of 7.5 mm. It can be noted that the resistance slightly increases with the reduction of tensile radius in both substrates. After each bent measurement, the samples were released and measured in flat position, where the values remain similar to the original flat position measurements. This indicates that there is no degradation in the silver paths during the mechanical stress. These reliable results open the opportunity to explore the use of 3D printed shadow masks in Flexible PCBs applications. Recently, the research community is interested in the challenges of manufacturing biodegradable PCBs and their novel applications in devices and sensors [36]. The use of recyclable substrates such as PET and paper fulfils the requirements for these applications.

TABLE I. Resistance of the silver paths on different substrates varying the tensile radius systematically.

Substrate	Flat Position	17.5 mm	15 mm	12.5 mm	10 mm	7.5 mm
PET	$5.7 \pm 0.1~\Omega$	$5.7 \pm 0.2~\Omega$	$5.7\pm0.2\Omega$	$5.9 \pm 0.2~\Omega$	$6.0\pm0.3~\Omega$	$6.2\pm0.3\Omega$
Paper	$15.1 \pm 0.4~\Omega$	$15.1\pm0.4~\Omega$	$15.2 \pm 0.4~\Omega$	$15.4 \pm 0.4~\Omega$	$15.7\pm0.5~\Omega$	$15.9 \pm 0.5~\Omega$

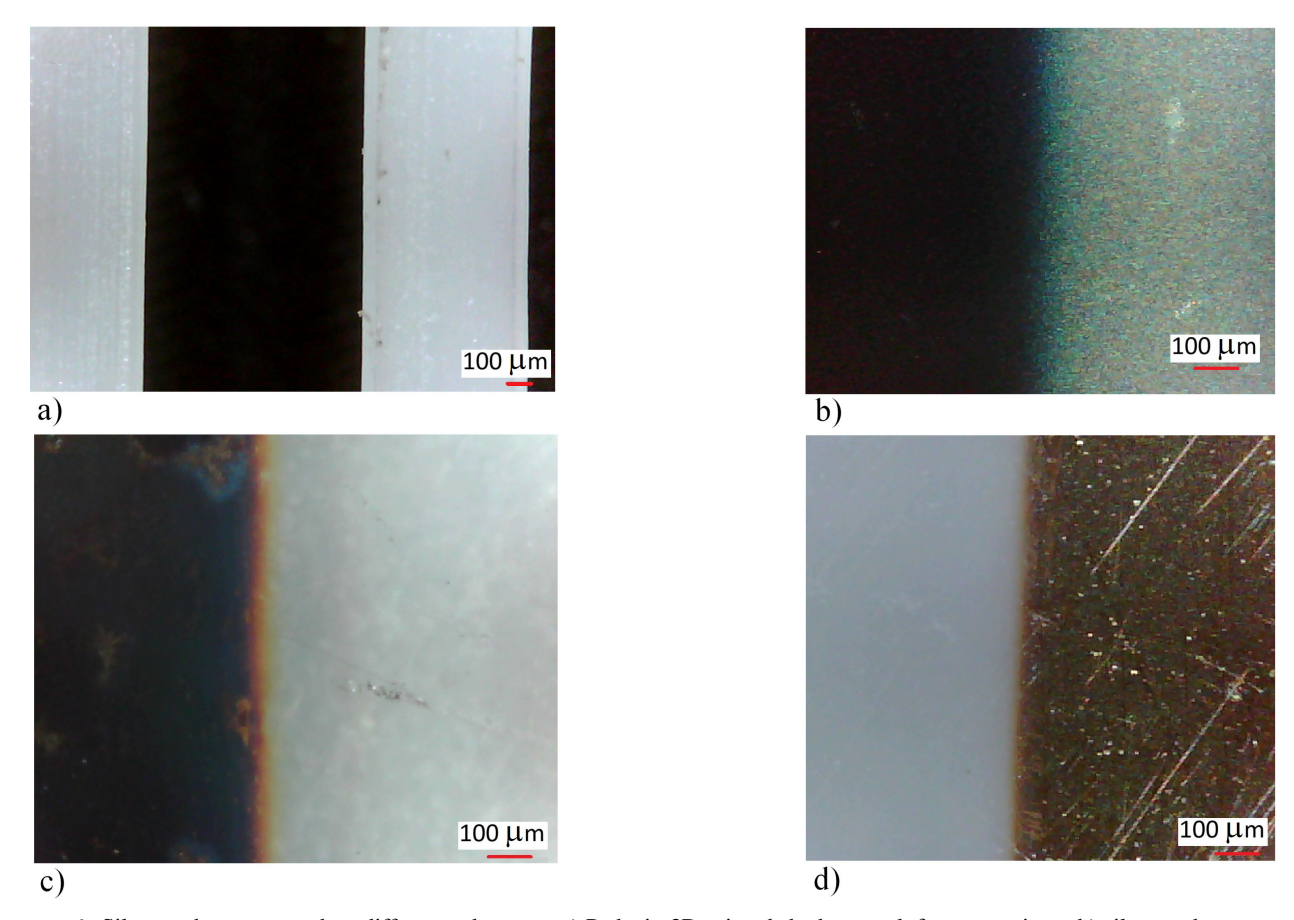


FIGURE 6. Silver paths evaporated on different substrates. a) Paths in 3D printed shadow mask for comparison. b) silver paths evaporated on silicon wafers. c) silver paths on PET substrates. d) silver paths on photographic paper.

To demonstrate a flexible PCB application, a silver path evaporated on PET substrate is used as a transmission line for a sine electrical signal. The selected electrical characteristics were just as an example. The flexible PCB is under operation in flat and bent positions. Figure 8a) shows the schematic

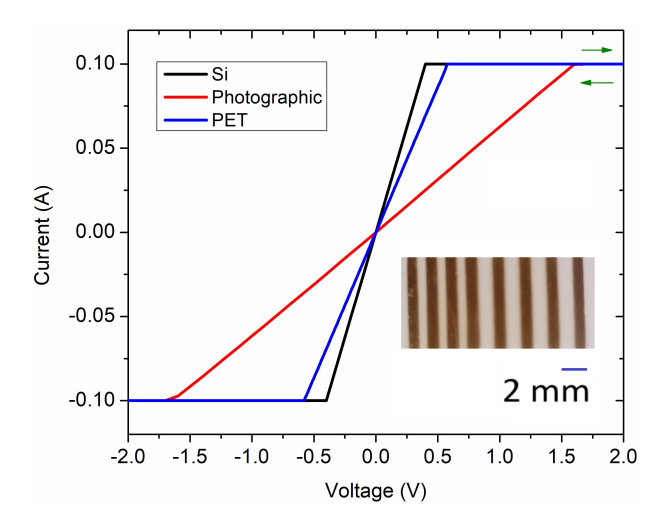


FIGURE 7. Forward and reverse current-voltage measurements of the silver paths on different substrates. Inset: Photograph of the silver paths on photographic paper.

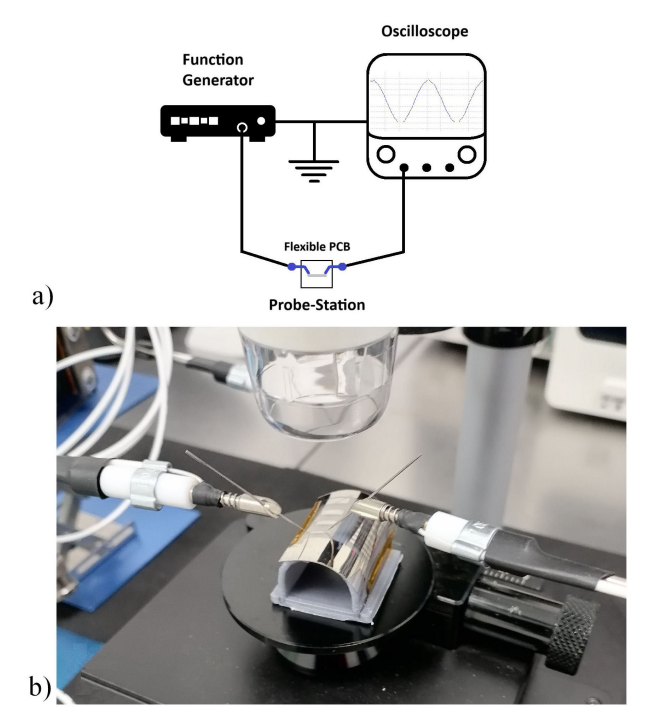


FIGURE 8. Demonstration of a transmission line in flexible PCB applications. a) Schematic representation of the test and measurements setup. b) Bent sample using a 3D printed device with a tensile radius of 7.5 mm.

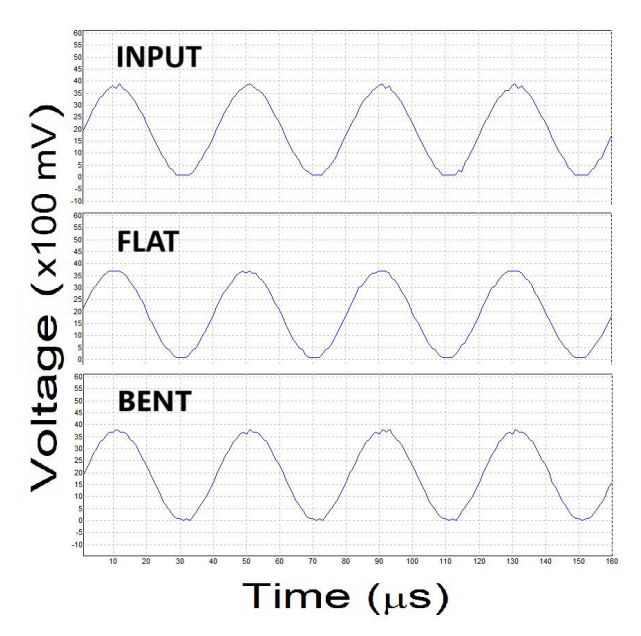


FIGURE 9. Electrical measurements of the transmission line in flat and bent positions. The input signal is shown for comparison.

representation of the test and measurements setup, and Fig. 8b) shows the bent sample using a 3D printed device with a tensile radius of 7.5 mm. Figure 9 shows the electrical measurements of the transmission line in flat and bent positions, the input signal is shown for comparison. These results indicate that there is no signal loss or attenuation in the transmission line, even when the flexible PCB is bent and returned to flat position. The sine signal was switched to triangular and square signals with similar results (not shown here), as expected. Moreover, the initial frequency was 10 kHz and was increased to 200 kHz with no attenuation or signal loss. Therefore, it can be concluded that 3D printing for microfabrication in flexible PCBs meets successfully the requirements to enable flexible novel applications.

On the other hand, as a future perspective, the 3D printed shadow mask also can be used to transfer metal patterns as contacts into flexible electronic devices and to evaluate device parameters such as contact resistance in field-effect transistors [37]. The contact resistance can be extracted by the extrapolation of the width-normalized resistance (obtained from the linear regime of Ids vs Vds) for different channel lengths and gate voltages Vgs; the design depicted in fig 2 can

be useful for this purpose and also, can be used to evaluate the Transfer Length Method (TLM) which consist in currentvoltage measurements of contacts at different separation [38].

Based on the results shown in this work, 3D printing can find a reliable use for microfabrication and mechanical stress characterization in flexible electronics. 3D printing offers unlimited possible designs that can be adapted to the requirements of every single application and can enable several novel applications in flexible electronics.

4. Conclusions

In this work, the application of 3D printing for microfabrication and mechanical stress characterization in flexible electronics is presented. In mechanical stress characterization, the 3D printed device shows accuracy, versatility and easy implementation in any probe-station for characterization during operation of the electronic devices. The PLA 3D shadow mask successfully transferred silver patterns to flexible substrates such as PET and photographic paper. The currentvoltage measurements of the silver paths exhibit linear, symmetric behavior and negligible hysteresis. The optimal minimum length was found in 600 μ m, this resolution is reliable for Flexible PCBs and may be efficient for fast fabrication in flexible electronic devices. The demonstration of a flexible PCB application is shown. The transmission line did not show signal loss or attenuation, even when the flexible PCB is bent with a tensile radius of 7.5 mm.

Acknowledgments

The authors want to thank the personnel of the Flexible Electronics Research Lab at Ecocampus-BUAP for the 3D printing and flexible electronic microfabrication. AGG would like to thank to Programa Delfín-Verano de la Investigación Científica y Tecnológica del Pacífico for the research stay support.

Funding

This work was partially supported by Fondo Sectorial de Investigación para la Educación [A1-S-7888] and Proyectos VIEP-BUAP.

^{1.} K. Natu, M. Laad, B. Ghule and A. Shalu, Transparent and flexible zinc oxide-based thin-film diodes and thin-film transistors: A review. *J. Appl. Phys.*, **134** (2023) 190701, https://doi.org/10.1063/5.0169308

^{2.} P. Bhat, P. Salunkhe and D. Kekuda, Flexible ultraviolet photosensors based on p-NiO/n-Zn(1-x)Sn(x)O heterojunction with an ZnO interfacial layer that works in self regime mode. *Sensors & Actuators A: Physical* **354** (2023) 114279, https:

^{//}doi.org/10.1016/j.sna.2023.114279

^{3.} A. Panca, J. Panidi, H. Faber, S. Stathopoulos, T. Anthopoulos and T. Prodromakis, Flexible Oxide Thin Film Transistors, Memristors, and Their Integration. *Adv. Funct. Mater.*, **33** (2023) 2213762, https://doi.org/10.1002/adfm. 202213762

M. Petrelli et al., Flexible Sensor and Readout Circuitry for Continuous Ion Sensing in Sweat. IEEE Sensors Lett., 7 (2023)

- 550180,4 https://doi.org/10.1109/LSENS.2023.3274682
- M. Dominguez and J. Sosa, Copper phthalocyanine buffer interlayer film incorporated in paper substrates for printed circuit boards and dielectric applications in flexible electronics. *Solid State Electron.*, 172 (2020) 107898, https://doi.org/10.1016/j.sse.2020.107898
- M. Dominguez, J. Pau and A. Redondo, Flexible Zinc Nitride Thin-Film Transistors Using Spin-On Glass as Gate Insulator. *IEEE Trans. Electron Devices*, 65 (2018) 1014, https: //doi.org/10.1109/TED.2018.2797254
- J. Sheng, H. Jeong, K. Han, T. Hong and J. Park, Review of recent advances in flexible oxide semiconductor thin-film transistors. *J. Inf. Display*, 18 (2017) 159, https://doi.org/ 10.1080/15980316.2017.1385544
- 8. M. Dominguez, J. Luna and S. Ceron, Low-temperature ultrasonic spray deposited aluminum doped zinc oxide film and its application in flexible Metal-Insulator-Semiconductor diodes. *Thin Solid Films*, **645** (2018) 278, https://doi.org/10.1016/j.tsf.2017.11.006
- 9. S. Wang, C. Yeh, C. Hsu and J. Lou, Fabricating Thin-Film Transistors on Plastic Substrates Using Spin Etching and Device Transfer. *J. Electrochem. Soc.*, **152** (2005) G227, https://doi.org/10.1149/1.1860491
- P. Schlupp, S. Vogt, H. Wenckstern and M. Grundmann, Low voltage, high gain inverters based on amorphous zinc tin oxide on flexible substrates. *APL Mater.*, 8 (2020) 061112 https: //doi.org/10.1063/1.5143217
- 11. Y. Fu *et al.*, Superflexible inorganic Ag2Te0.6S0.4 fiber with high thermoelectric performance. *Advanced Science*, **10** (2023) e2207642, https://doi.org/10.1002/advs. 202207642
- 12. D. Rocha *et al.*, Posttreatment of 3D-printed surfaces for electrochemical applications: A critical review on proposed protocols. *Electrochem. Sci. Adv.*, **2** (2022) e2100136, https://doi.org/10.1002/elsa.202100136
- 13. M. Palacios, M. Sanna, J. Muñoz, K. Ghosh, S. Wert and M. Pumera, Heterolayered carbon allotrope architectonics via multi-material 3D printing for advanced electrochemical devices. *Virtual and Physical Prototyping*, **18** (2023) e2276260, https://doi.org/10.1080/17452759.2023.2276260
- 14. C. Kim, C. Sullivan, A. Hillstrom and R. Wicker, Intermittent embedding of wire into 3D prints for wireless power transfer. *International Journal of Precision Engineering and Manufacturing*, **22** (2021) 919, https://doi.org/10.1007/s12541-021-00508-y
- 15. S. Ali, I. Deiab and S. Pervaiz, State-of-the-art review on fused deposition modeling (FDM) for 3D printing of polymer blends and composites: innovations, challenges, and applications. *International Journal of Advanced Manufacturing Technology*, **135** (2024) 5085, https://doi.org/10.1007/s00170-024-14820-0
- L. Guterres, C. Costa, A. Tanaka, L. Ferreira, I. Santos, and J. Santos, Electrochemical Biosensors 3D Printed by Fused Deposition Modeling: Actualities, Trends, and Challenges. *Biosensors*, 15 (2025) 57, https://doi.org/10.3390/ bios15010057

- 17. N. Sowmya, N. Oraon, S. Sen and M. Rao, Development of 3D shadow mask using 3D printer. In *IEEE CONECCT*, 2015, https://doi.org/10.1109/CONECCT.2015.7383925
- S. Rahiminejad, E. Kohler and P. Enoksson, Direct 3D printed shadow mask on Silicon. *Journal of Physics: Conference Se*ries, 757 (2016) 012021 https://doi.org/10.1088/ 1742-6596/757/1/012021
- 19. M. Keough *et al.*, Realizing new designs of multiplexed electrode chips by 3-D printed masks. *RSC Advances*, 11 (2021) 21600-21606 https://doi.org/10.1039/D1RA03482K
- S. Khan, W. Dang, L. Lorenzelli and R. Dahiya, Printing of High Concentration Nanocomposites (MWNTs/PDMS) Using 3D-Printed Shadow Masks. In AISEM Conference, 2015, https://doi.org/10.1109/AISEM.2015. 7066786
- 21. J. Jang, K. Cho, S. Lee and S. Kim, Transparent and flexible thin-film transistors with HgTe nanocrystals. *Nanotechnology*, **19** (2008) 015204, https://doi.org/10.1088/0957-4484/19/01/015204
- 22. X. Liu *et al.*, Implementing Room-Temperature Fabrication of Flexible Amorphous Sn-Si-O TFTs via Defect Control. *Advanced Materials Interfaces*, **8** (2021) 2002193, https://doi.org/10.1002/admi.202002193
- 23. T. Carey *et al.*, High-Mobility Flexible Transistors with Solution-Processed Tungsten Dichalcogenides. *ACS Nano*, **17** (2023) 2912, https://doi.org/10.1021/acsnano. 2c11319
- 24. A. Zumeit, A. Dahiya, A. Christou, R. Mukherjee and R. Dahiya, Printed GaAs Microstructures-Based Flexible Photodetectors. Advanced Materials Technologies, 7 (2022) 2200772, https://doi.org/10.1002/admt. 202200772
- Z. Ahmadi, S. Lee, A. Patel, R. Unocic, N. Shamsaei and M. Mahjouri-Samani, Dry Printing and Additive Nanomanufacturing of Flexible Hybrid Electronics. *Advanced Materials Interfaces*, 9 (2022) 2102569, https://doi.org/10.1002/admi.202102569
- 26. X. Zhang *et al.*, Review on flexible perovskite photodetector: processing and applications. *Frontiers of Mechanical Engineering*, **18** (2023) 33, https://doi.org/10.1007/s11465-023-0749-z
- 27. A. Nawaz, L. Merces, L. Ferro, P. Sonar and C. Bufon, Impact of Planar and Vertical Organic Field-Effect Transistors on Flexible Electronics. *Advanced Materials*, **35** (2023) 2204804, https://doi.org/10.1002/adma.202204804
- 28. A. Katiyar *et al.*, 2D Materials in Flexible Electronics: Recent Advances and future prospectives. *Chemical Reviews*, **124** (2024) 318, https://doi.org/10.1021/acs.chemrev.3c00643
- 29. Q. Zhang *et al.*, Flexible wearable energy storage devices: Materials, structures and applications. *Battery Energy*, **3** (2024) 20230061, https://doi.org/10.1002/bte2.20230061

- 30. M. Wei *et al.*, Directional Thermal Diffusion Realizing Inorganic Sb₂Te₃/Te Hybrid Thin Films with High Thermoelectric Performance and Flexibility. *Advanced Functional Materials*, **32** (2022) 2207903, https://doi.org/10.1002/adfm.202207903
- 31. X. Shi *et al.*, Advances in flexible inorganic thermoelectrics. *EcoEnergy*, **1** (2023) 296, https://doi.org/10.1002/ece2.17
- 32. E. Alexandre, T. Beduk, S. Lengger, M. Vijjapu, S. Carrara and J. Kosel, Glucose sensor printed on algae-based substrates for eco-conscious point-of-care devices. *IEEE Sensors Letters*, **9** (2025) 4500204 https://doi.org/10.1109/LSENS. 2024.3505959
- P. Nair, V. Santurkar, K. Amreen, R. Ponnalagu and S. Goel, Gold/Cerium(IV) Oxide-Modified Flexible Electrodes for Enzymatic Detection of Triglyceride. *IEEE Sensors Letters*, 8 (2024) 4504704 https://doi.org/10.1109/LSENS. 2024.3506160
- 34. Y. Guo *et al.*, Fully Flexible Integrated and Self-Powered Smart Bending Strain Skin for Wireless Monitoring of Heavy Industrial Equipment. *IEEE Transactions on Instrumentation*

- and Measurement, 74 (2025) 2502012, https://doi.org/ 10.1109/TIM.2024.3502818
- 35. L. Marini, S. Dinesh, S. Jhajharia, M. Padmanabhan, R. Mahajan and P. Chithra, Screen Printable, Sustainable Water-Based Functional Ink From Coal-Derived Reduced Graphene Oxide for Humidity Sensing. *IEEE Sensors Letters*, **9** (2025) 2000204, https://doi.org/0.1109/LSENS.2024.3510873
- C. Soon *et al.*, Advancements in Biodegradable Printed Circuit Boards: Review of Material Properties, Fabrication Methods, Applications and Challenges. *Int. J. Precis. Eng. Manuf.*, 25 (2024) 1925, https://doi.org/10.1007/s12541-024-01027-2
- 37. M. Dominguez, J. Pau, M. Gómez, J. Luna and P. Rosales, High mobility thin film transistors based on zinc nitride deposited at room temperature. *Thin Solid Films*, **619** (2016) 261, https://doi.org/10.1016/j.tsf.2016.10.053
- 38. M. Dominguez *et al.*, Planarized ambipolar a-SiGe:H thin-film transistors: Influence of the sequence of fabrication process. *Solid State Electron.*, **99** (2014) 45, https://doi.org/10.1016/j.sse.2014.06.024